Thermal characteristic of sintered Ag–Cu nanopaste for high-temperature die-attach application

Kim Seah Tan [a], Yew Hoong Wong [b], Kuan Yew Cheong [a, *]

[a] Electronic Materials Research Group, School of Materials and Mineral Resources Engineering, Universiti Sains Malaysia, Engineering Campus, 14300 Nibong Tebal, Penang, Malaysia
[b] Department of Mechanical Engineering, Faculty of Engineering, Universiti Malaya, 50603 Kuala Lumpur, Malaysia

ARTICLE INFO

Article history:
Received 6 November 2013
Received in revised form
3 August 2014
Accepted 26 August 2014
Available online 22 September 2014

Keywords:
Melting temperature
Thermal conductivity
Coefficient of thermal expansion
Performance index
Sintering

ABSTRACT

In this work, thermal characteristic of silver–copper (Ag–Cu) nanopaste that consists of a mixture of nano-sized Ag and Cu particles and organic compounds meant for high-temperature die-attach application is reported. The Ag–Cu nanopaste was sintered at 380 °C for 30 min without the need of applying external pressure and the effect of Cu loading (20–80 wt%) on the thermal properties was investigated in against of pure Ag nanopaste and pure Cu nanopaste. The results showed the specific heat of sintered Ag–Cu nanopaste was increased as the loading of Cu increased. For thermal conductivity and coefficient of thermal expansion (CTE) of sintered Ag–Cu nanopaste, a declining trend has been recorded with the increment of Cu loading. Overall, the sintered Ag–Cu nanopaste with 20 wt% of Cu loading has demonstrated the best combination of thermal conductivity (K) and CTE (α), which were 159 W/m K and 13×10^{-6}/K, respectively. It has proven that there was a strong correlation between the amount of pores and thermal properties of the nanopaste. The ratio of K/α is a performance index (M), which has shown a higher value (12.2×10^6 W/m) than most of the commonly used die-attach systems. Finally, the Ag–Cu nanopaste has demonstrated a melting point of 955 °C, which can be proposed as an alternative high-temperature die-attach material.

1. Introduction

In recent years, electronic devices are continually improving for high-temperature applications, such as (i) brake and exhaust gas sensors for automotive (500–1000 °C) [1], (ii) turbine and gas sensors for aeronautic (~600 °C) [2], (iii) geothermal sensor for well-logging (~600 °C) [3], (iv) nuclear radiation detector and nuclear reactor for nuclear plant (700–1000 °C) [2,4], and (v) transmitter, antenna and electromechanical devices for space exploration (>500 °C) [5]. The challenge is thus driven to design an electronic packaging material, i.e. die-attach material, that is able to work in the aforementioned high-temperature conditions. The primary focus is therefore aimed to select a die-attach material that possesses melting point higher than 500 °C, which makes it suitable for high-temperature applications [6]. In addition, the die-attach material must also possess high thermal conductivity to dissipate the heat that originating from the die to the substrate [6], as well as, possess low coefficient of thermal expansion (CTE) to minimize the buildup strain that caused by temperature gradient [6]. To relate both thermal conductivity and CTE, performance index is thus being used to optimize the selection of a die-attach material. According to Fourier's Law for steady state one directional, x, heat flow from die to substrate [7]:

$$q = \frac{K}{x}\Delta T \tag{1}$$

where q is the heat input per unit area, K is the thermal conductivity, and ΔT is the change of temperature. The buildup strain, ε, in the die-attach material is related to the change of temperature by [7]:

$$\varepsilon = \alpha \Delta T \tag{2}$$

where α is the CTE. Eq. (3) is thereby derived by combining Eqs. (1) and (2) [7]:

$$q = \frac{\varepsilon}{x}\left(\frac{K}{\alpha}\right) \tag{3}$$

* Corresponding author. Tel.: +60 4 5995259; fax: +60 4 5941011.
E-mail addresses: srcheong@usm.my, ckuanyew@yahoo.com (K.Y. Cheong).

http://dx.doi.org/10.1016/j.ijthermalsci.2014.08.022
1290-0729/

Thus, for a given heat flow from the die, the buildup strain (ε) could be minimized by selecting a die-attach material with large value of K/α, which is defined as performance index, M [7]:

$$M = \frac{K}{\alpha} \tag{4}$$

The larger value of performance index indicates the die-attach material has higher efficiency in conducting thermal energy from the die to the substrate, making less thermal energy being absorbed and stored in the atoms of die-attach material. Less thermal energy being stored will eventually cause less displacement of the inter-atomic distance, which resulting less deformation of the die-attach material. With this idea in mind, the performance indices for various die-attach materials are being computed for later comparison (Table 1).

In general, die-attach materials can be classified into five categories, which are conductive adhesive, solder alloy, conductive glass, metal film, and metal paste (Fig. 1). Nowadays, conductive adhesive [8–10] and tin (Sn) based solder alloys (lead-bearing and lead-free) [11–14] are most commonly used die-attach materials for level-1 interconnection, namely between the die and substrate, but these materials are having low value of M (0.1–1.8 $\times$ 10^6 W/m) (Table 1) and low melting points (<250 °C), making them only suitable to be applied for low-temperature range (≤300 °C) of applications (Fig. 1) [6]. Conductive glass [15], gold (Au) [12,15–17], bismuth (Bi) [18–20], and zinc (Zn) [21–23] based solder alloys were subsequently introduced. But most of these materials are also displaying low value of M (2.3–3.9 $\times$ 10^6 W/m) (Table 1) with maximum melting point at 400 °C, which limited to application at medium-temperature range (300–500 °C) (Fig. 1) [6]. Although Au-nickel (Ni) is an exceptional solder alloy that could be operated at high-temperature range (≥500 °C) but its high soldering temperature at 980 °C has become a drawback [24]. Metal film and metal paste systems are next being introduced, which aim to reduce the processing temperature, yet the entire system still able to operate at medium to ultra-high temperature ranges. Au–Au [25], Au-indium (In) [26], and silver (Ag)–In [27] are particular systems that form a joint by inter-diffusion bonding of metal films at temperature of 200–300 °C and pressure of 0.28–40 MPa. The joints formed by Au–Au and Ag–In films could be operated at ultra-high temperature range (≥700 °C), whereas the joint formed by Au–In film is only limited to medium-temperature range (300–500 °C) (Fig. 1). However, this inter-diffusion bonding technique requires additional long annealing duration (26–100 h) in order to increase its bonding strength [26,27]. Au [25], Ag [28] and copper (Cu) [29] micropastes are next sourcing as alternative solutions. These micropastes (i.e. a mixture of micro-sized metal particles and organic compounds) utilize sintering technique to form a joint at temperature of 700 °C; whilst application of external pressure (40 MPa) in assists of sintering process could further lower the sintering temperature down to 250 °C [25,28,29]. The joint formed by sintering of metal micropaste technique, with or without pressure assisted, has been proven suitable for ultra-high temperature range (≥700 °C) of applications with melting point higher than 960 °C (Fig. 1) [25,28,29]. But the application of external pressure during sintering tends to complicate the manufacturing process. Ag hybrid micro-nanopaste [30,31] (i.e. a mixture of micro- and nano-sized metal particles and organic compounds), Ag nanopaste [32–36] and Cu nanopaste [37] (i.e. a mixture of nano-sized metal particles and organic compounds) were then introduced to promote sintering at 250–380 °C without the need of external pressure in assisting the sintering process.

Ag, however, is limited to its high cost and low electrochemical migration resistance [38–40]; whereas Cu is limited to its complicated die-attach process, such as the requirement to preheat at vacuum atmosphere prior to sintering, and the sintering process must carry out in either H_2/N_2 or vacuum atmosphere [37]. The sintered Cu nanopaste even required additional 4 h annealing at N_2 atmosphere to minimize oxidation of Cu [37]. As a result, two alternative materials that could be used at high-temperature range, namely Ag–Al [41] and Ag–Cu [42,43] nanopastes, were introduced to surpass the preceding limitations of Ag and Cu nanopastes. These materials not only could tailor the cost to be cheaper than Ag nanopaste, yet it could also sinter in air atmosphere without assisting of external pressure and additional annealing step, hence making the die-attach process becomes much simpler. By comparing between Ag–Al and Ag–Cu nanopastes, Ag–Cu nanopaste that was studied in our previous works [42,43] has

Table 1
Thermal conductivity, CTE and performance index for various die-attach systems.

Die-attach system	Thermal conductivity, K (W/m K) at 25 °C	CTE, α ($\times 10^{-6}$/K)	$M = K/\alpha$ ($\times 10^6$ W/m)	Ref.
Metal paste				
(i) Ag nanopaste	200–240	19–20	10.0–12.6	[33,34,36]
(ii) Ag–Cu nanopaste	159	13	12.2	This work
(iii) Ag–Al nanopaste	123	8	15.4	[41]
(iv) Ag hybrid paste	136–250	19.7*	6.9–12.7	[30,31]
(v) Cu micropaste	94	16.5*	5.7	[29]
(vi) Ag micropaste	80–220	19.7*	4.1–11.2	[28,32]
Metal film				
(i) Au	–	–	–	[25]
(ii) Au–In	–	–	–	[26]
(iii) Ag–In	–	–	–	[27]
Conductive glass	60–80	16–25	2.4–5.0	[15]
Solder alloy				
(i) Zn	77–110	20–30	3.7–3.9	[21–23]
(ii) Au	27–59	12–16	2.3–3.7	[15–17]
(iii) Sn				
(a) Pb-free	20–66	15–40	1.3–1.7	[11,12,14,16,36]
(b) Pb-bearing	23–53	19–30	1.2–1.8	[11,12,14,22,36]
(iv) Bi	7–11	–	–	[18,19]
Conductive adhesive	1–25	26–53	0.1–0.5	[8]

Symbol "–" means no reported value. Symbol "*" is theoretical value.

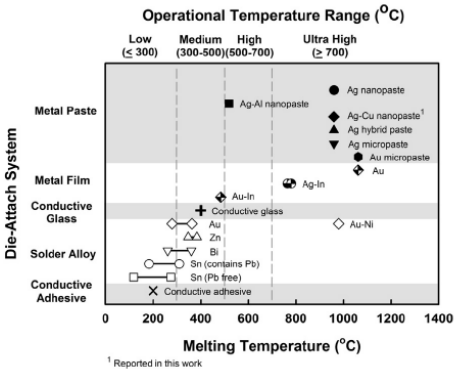

Fig. 1. Melting temperature of various die-attach systems and their operational temperature range [6,8–37,41].

offered a better electrical conductivity, higher bonding strength, and better corrosion resistance than Ag–Al nanopaste. This makes Ag–Cu nanopaste a potential candidate for high and ultra-high temperature applications. However, detail understanding of the thermal behavior of this system has yet been reported. Therefore, in this work, thermal properties of Ag–Cu nanopaste have been systematically presented. It is shown that Ag–Cu nanopaste is having the fourth highest value of performance index (12.2×10^6 W/m) if compared to other metal pastes ($4.1–12.7 \times 10^6$ W/m) (Table 1). Although Ag–Al nanopaste displays the highest value of performance index (15.4×10^6 W/m) (Table 1), yet its melting point (519 °C) is drastically lower than the melting point of Ag–Cu nanopaste (955 °C) (Fig. 1). This makes Ag–Cu nanopaste become a promising alternative die-attach material for high to ultra-high temperature applications.

2. Experimental details

Ag and Cu nanoparticles were acquired commercially from MTI Corp., Richmond, USA, with average sizes of 40 ± 10 nm and 50 ± 10 nm, respectively. The nanopaste was prepared by mixing both Ag and Cu nanoparticles with an organic binder and solvent system, which constituted of resin binder (V006 from Heraeus, Inc.), terpineol (RV372 from Heraeus, Inc.) and ethylene glycol (MW 40,000 from Merck). The total weight percent (wt%) of the metal nanoparticles content (Ag and Cu combined) within the nanopaste was kept at 87 wt% [41,43]. The ratio of Cu content was varied from 20, 40, 50, 60 to 80 wt% with respect to Ag content, in order to study its effect on the thermal characteristic of nanopaste. Pure Ag nanopaste and pure Cu nanopaste were also prepared as control samples by using the same formula. The nanopaste was stencil printed onto pre-cleaned soda lime glass substrate with stencil thickness of 50.8 μm and area of 1.0 × 1.0 cm^2. A Lenton horizontal tube furnace was used to sinter the printed nanopaste in open air at 380 °C with a ramp rate of 5 °C/min and dwell time of 30 min [42]. After this, the furnace was naturally cooled down to room temperature before the sintered nanopaste was being withdrawn from the furnace.

The sintered nanopaste was scratched off from the soda lime glass and used for subsequent thermal analysis. Differential scanning calorimetry (DSC) (Mettler Toledo 1 STAR) was used to determine the specific heat and melting temperature of the sintered nanopaste. For specific heat measurement, a baseline balancing procedure was used [44]. The DSC test was carried out under nitrogen purge, where the thermal program began with isothermally held at 25 °C for 3 min, followed by ramping at 10 °C/min from 25 to 300 °C, and end with isothermally held at 300 °C for 3 min. This thermal program setting was first measured with empty aluminum pans. The same setting was then repeated for respective 15 ± 1 mg of pure Ag reference standard and sintered nanopaste samples. The specific heat of the sintered nanopaste was then calculated according to Eq. (5).

$$C_{p1} = \frac{m_2 y_1}{m_1 y_2} C_{p2} \tag{5}$$

where C_{p1} and C_{p2} are specific heat of the sintered nanopaste sample and the reference standard, respectively; m_1 and m_2 are mass of the sintered nanopaste sample and reference standard, respectively; and y_1 and y_2 are the net heat flow of the sintered nanopaste sample and reference standard, respectively. For melting point measurement, the DSC test was carried out under nitrogen purge using a ramp rate at 10 °C/min from 25 to 1000 °C.

For subsequent characterization, the prepared nanopaste was vacuum evaporated to remove the excess organic solvent, followed by forming it into disc-shape nanopaste sample with diameter of 12.7 mm and thickness of 2.0–3.0 mm. This disc-shape nanopaste sample was prepared by using a mold-die set and hydraulic press. A pressure of 1500 psi (10.34 MPa) was used to compact the nanopaste into green body to simulate the actual pressure applied upon the die placement and attachment process on a die-attach material [41,45]. Next, the green body was removed from the mold-die. A Lenton horizontal tube furnace was used to sinter the green body in according to the aforementioned sintering profile. The disc-shape sample was prepared in accordance to Refs [33,34,41], but there might be difference of microstructure between the disc-shape sample and thin layer sample, which may cause variation in measurement. The bulk density and porosity were measured by Archimedes method using disc-shape sintered nanopaste sample. The thermal diffusivity was measured using Netzsch LFA-447 Nanoflash laser system, wherein the sintered disc-shape nanopaste sample (thickness of 2.0–2.2 mm) was rapidly heated on one side of the sample surface at 25, 150 and 300 °C, and the temperature rise on the opponent side of sample surface was measured. The thermal conductivity (K) of the sintered nanopaste was then calculated using Eq. (6) with the obtained specific heat (C_{p1}), bulk density (ρ) and thermal diffusivity (λ).

$$K = \rho C_{p1} \lambda \tag{6}$$

The thermal expansion for the sintered disc-shape nanopaste sample (thickness of ~3.0 mm) was measured from 25 to 300 °C at a ramp rate of 5 °C/min using a Perkin–Elmer Diamond thermo-mechanical analysis system. The coefficient of thermal expansion (CTE) (α) for the sintered nanopaste was calculated using Eq. (7).

$$\alpha = \frac{\Delta L}{L_0 \Delta T} \tag{7}$$

where ΔL is change of the sample length, L_o is original sample length and ΔT is change of the temperature.

3. Results and discussion

3.1. Melting point and safety operating temperature

Fig. 2 depicts DSC curves for sintered pure Ag nanopaste (0 wt% Cu), sintered pure Cu nanopaste (100 wt% Cu) and sintered Ag–Cu

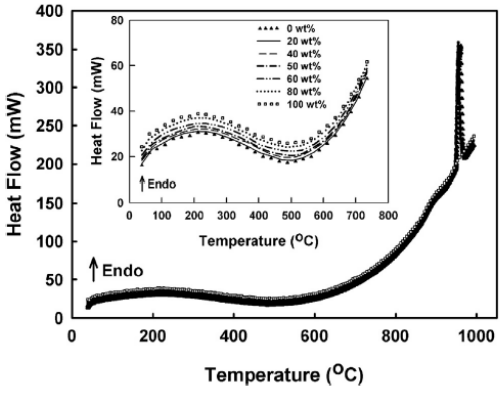

Fig. 2. DSC curves for sintered pure Ag nanopaste (0 wt% Cu), sintered pure Cu nanopaste (100 wt% Cu) and Ag–Cu nanopaste with various Cu loadings (20–80 wt% Cu). Inset resolves the overlapped curves.

nanopaste with various Cu loadings (20–80 wt% Cu), in which the curves are found overlapped to each other. The overlapped curves are being resolved in the inset of Fig. 2, and it shows that the curve is shifted to a higher endothermic heat flow with the increment of Cu loading. From Fig. 2, an obvious and sharp endothermic peak is revealed at a temperature of about 955 °C, where it is associated as the melting temperature (T_m) of sintered Ag–Cu nanopaste. There is another sharp endothermic peak is revealed at temperature of 962 °C, where it represents the T_m of pure Ag nanopaste. Nonetheless, due to the limitation of the machine to perform the test up to a maximum temperature of 1000 °C, Fig. 2 could not reveal any peak for pure Cu nanopaste which estimates to be melted at a temperature of 1085 °C. This estimation has been made because of the pure Ag nanopaste is melted at a temperature that is same as its theoretical value (962 °C) [46]; hence, we predict that pure Cu nanopaste might be the same, which could be melted at its theoretical T_m (1085°) [46]. The T_m of the sintered Ag–Cu nanopaste (955 °C) is slightly lower than that of pure Ag nanopaste (962 °C) and pure Cu nanopaste (1085 °C). According to the Ag–Cu binary phase diagram [47,48], the reduction of T_m may due to the formation of Ag–Cu compound ($Ag_{97}Cu_3$) [43] that is having a lower T_m (955 °C) than pure Ag (962 °C) and pure Cu (1085 °C). On the other hand, the enthalpy of melting for sintered nanopaste is being extracted from the area under the peak, where 120 and 110 J/g are revealed for Ag–Cu nanopaste and pure Ag nanopaste, respectively. The enthalpy of melting for sintered Ag–Cu nanopaste is considerably larger than the value of Sn based solder alloys (7–69 J/g) [49–52]. This indicates that a large amount of energy is required to melt the sintered Ag–Cu nanopaste. But the enthalpy of melting for Ag–Cu nanopaste is lower than that of Ag–Al nanopaste (186 J/g) [53]. Besides, Fig. 1 depicts the T_m of various die-attach systems in against of Ag–Cu nanopaste. Although the Ag–Cu nanopaste is not having the highest T_m amongst other die-attach systems, yet its T_m (955 °C) is still high enough for application in high to ultra-high temperature range (>500 °C). In addition, a safety operating temperature (T_o), also known as maximum operating temperature, needs to be determined in order to allow the nanopaste to be used as a die-attach material in a practical operating device. Therefore, a homologue temperature ratio (T_h) that typically set between 0.67 and 0.85 [45,54] was used to calculate the T_o in accordance to Eq. (8), where both T_m and T_o were calculated in unit Kelvin (K).

$$T_h = T_o / T_m \tag{8}$$

From the calculation, the Ag–Cu nanopaste is thus having a safety operating temperature range between 550 and 770 °C.

3.2. Specific heat, thermal diffusivity and thermal conductivity

Fig. 3(a) shows the DSC heat flow curves for empty pan, Ag reference standard, sintered pure Ag nanopaste (0 wt% Cu), sintered pure Cu nanopaste (100 wt% Cu) and sintered Ag–Cu nanopaste with various Cu loadings (20–80 wt% Cu). From these curves, the specific heat for sintered nanopaste is being computed from Eq. (5), and subsequently plotted in Fig. 3(b). Fig. 3(b) shows the specific heat of sintered Ag–Cu nanopaste is increasing from 0.27 to 0.34 J/g K, as the loading of Cu is increasing from 20 to 80 wt%. Moreover, sintered pure Ag nanopaste and sintered pure Cu nanopaste are having specific heat of 0.24 and 0.39 J/g K, respectively; whereby, these values are same as their bulk theoretical values [46] [represented by two horizontal lines in Fig. 3(b)]. The specific heat of sintered Ag–Cu nanopaste is thus lying between the specific heat, experimental and theoretical, of both Ag and Cu [Fig. 3(b)]. As the Cu loading in sintered Ag–Cu nanopaste is increasing from 20 to 80 wt%, its specific heat is deviating from Ag and approaching to Cu,

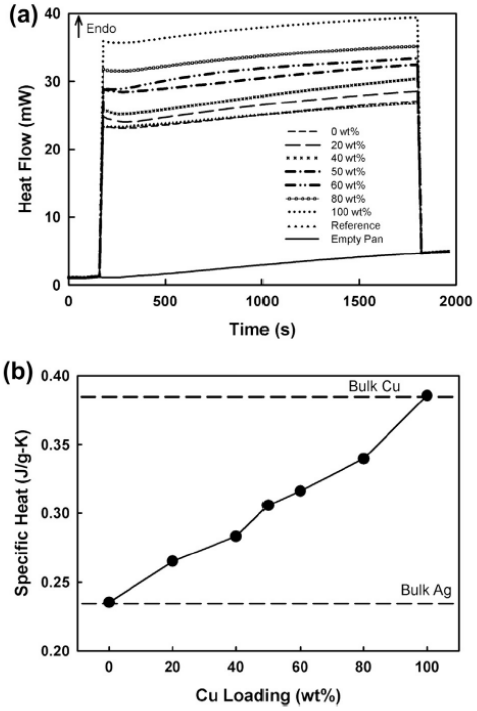

Fig. 3. (a) DSC heat flow curves for empty pan baseline, Ag reference standard, sintered pure Ag nanopaste (0 wt% Cu), sintered pure Cu nanopaste (100 wt% Cu) and sintered Ag–Cu nanopaste with various Cu loadings (20–80 wt% Cu); (b) specific heat for sintered pure Ag nanopaste (0 wt% Cu), sintered Cu nanopaste (100 wt% Cu) and sintered Ag–Cu nanopaste with increasing of Cu loading (20–80 wt% Cu).

indicating that a higher thermal energy is required to be absorbed and stored in order to raise the temperature of sintered Ag–Cu nanopaste.

Fig. 4(a) shows the thermal diffusivity for sintered pure Ag nanopaste (0 wt% Cu), sintered pure Cu nanopaste (100 wt% Cu) and sintered Ag–Cu nanopaste as a function of Cu loading (20–80 wt%) that measured at 25, 150 and 300 °C. The values of thermal diffusivity do not influence much by the measured temperature. This indicates that the sintered nanopaste is stable with elevated temperature and it is in agreement with the results shown in Section 3.1. From the plot at 25 °C, sintered pure Ag nanopaste and sintered pure Cu nanopaste have displayed thermal diffusivity values of 1.40 and 0.10 cm^2/s, respectively. Meanwhile, for sintered Ag–Cu nanopaste, a declining trend of the thermal diffusivity (1.18–0.17 cm^2/s) is observed as the Cu loading increases from 20 to 80 wt%. This declining trend could be related to the specific heat that has been reported in previous paragraph, in which a reversing trend of specific heat has been recorded [Fig. 3(b)]. When the Cu loading in sintered Ag–Cu nanopaste is increased, a higher thermal energy is being absorbed and stored in the atoms, as what has been elaborated in the previous paragraph, which resulting less thermal energy could be diffused through the sample. In addition, the thermal diffusivity value of sintered pure Ag nanopaste (1.40 cm^2/s) and sintered pure Cu nanopaste (0.10 cm^2/s) are lower than their respective bulk Ag (1.66 cm^2/s) and bulk Cu (1.11 cm^2/s) [46] [represented by two horizontal lines in Fig. 4(a)]. Furthermore,

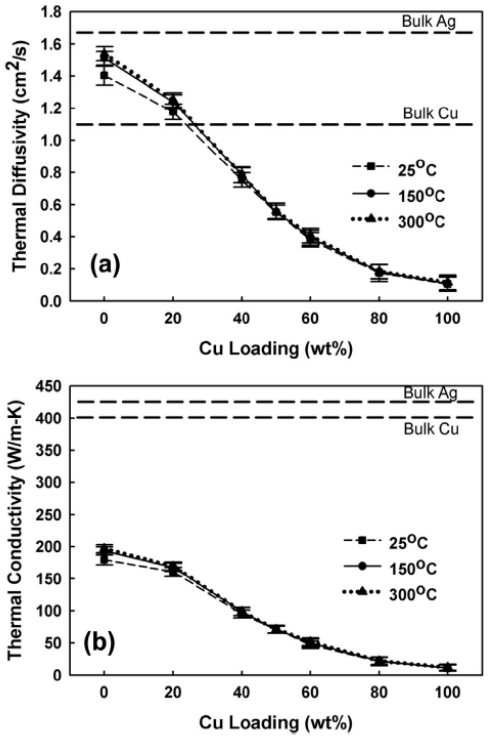

Fig. 4. (a) Thermal diffusivity and (b) thermal conductivity for sintered pure Ag nanopaste (0 wt% Cu), sintered pure Cu nanopaste (100 wt% Cu) and sintered Ag–Cu nanopaste with increasing of Cu loading (20–80 wt% Cu) at temperature 25, 150 and 300 °C.

the thermal diffusivity value of sintered Ag–Cu nanopaste (20–80 wt%) is also found to be lower than that of bulk Ag and bulk Cu, except for Ag–Cu nanopaste with 20 wt% of Cu loading which has displayed the value that is higher than bulk Cu [Fig. 4(a)]. The drop of thermal diffusivity may due to large amount of pores that presence in the Ag–Cu nanopaste, where the amount of porosity is increased from 50 to 62%, respectively, as the Cu loading is increased from 20 to 80 wt% [43]. The presence of pores in sintered nanopaste would be considered as defect centers, in which diffusion of thermal energy could be impeded due to absorption by the centers; thereby yielding a lower value of thermal diffusivity.

The thermal conductivity [Fig. 4(b)] of sintered pure Ag nanopaste (0 wt% Cu), sintered pure Cu nanopaste (100 wt% Cu) and sintered Ag–Cu nanopaste (20–80 wt%) are next computed by multiplying their respective thermal diffusivity with specific heat and bulk density in accordance to Eq. (6). The values of specific heat and bulk density have been reported in previous paragraph and in Ref. [43], respectively. From the plot at 25 °C, sintered pure Ag nanopaste and sintered pure Cu nanopaste have displayed thermal conductivity values of 179 and 11 W/m K, respectively. Meanwhile, the thermal conductivity value of sintered Ag–Cu nanopaste is reduced from 159 to 21 W/m K with the increment of Cu loading from 20 to 80 wt%. Since these values were computed from thermal diffusivity, the influence of measurement temperature is also insignificant. In the figure, two horizontal lines that represent the thermal conductivity values of bulk Ag (428 W/m K) and bulk Cu (401 W/m K) [46] are also shown for comparison. It has obviously seen that thermal conductivity value of sintered pure Ag nanopaste, sintered pure Cu nanopaste and sintered Ag–Cu nanopaste are much lower than the values of bulk Ag and bulk Cu. According to Eq. (6), thermal conductivity is determined by multiplying density, specific heat, and thermal diffusivity. These parameters are strongly influenced by the amount of pores that presence in a sample. Hence, the presence of 48 and 70% porosity in pure Ag nanopaste and pure Cu nanopaste, with no surprise, could eventually contribute to the reduction of thermal conductivity if compared to their bulk. In analogy, when the Cu loading in Ag–Cu nanopaste is increased from 20 to 80 wt%, the effect of increasing porosity from 50 to 62% [43] has also significantly contributed to the reduction of thermal conductivity if compared to bulk Ag and bulk Cu. Table 1 shows a comparison value of thermal conductivity of Ag–Cu nanopaste (20 wt% of Cu loading) in against other die-attach systems. Obviously, the thermal conductivity of Ag–Cu nanopaste (159 W/m K) is higher than most of the die-attach systems (1–123 W/m K), but it is still lower than Ag nanopaste (200–240 W/m K), Ag hybrid paste (136–250 W/m K), and Ag micropaste (80–220 W/m K).

3.3. Thermal expansion attribute

Fig. 5(a) shows the thermal expansion for sintered pure Ag nanopaste (0 wt% Cu), sintered pure Cu nanopaste (100 wt% Cu) and Ag–Cu nanopaste with various Cu loadings (20–80 wt% Cu). From each plot, there are two obvious slopes being recorded and differentiating these slopes is at a transition temperature. The transition temperature for thermal expansion is thus being determined and presented in Fig. 5(b), where the transition temperature is decreasing from 170 to 134 °C as the loading of Cu is increasing from 0 to 100 wt%. Fig. 5(c) shows the coefficient of thermal expansion (CTE) plots for sintered pure Ag nanopaste (0 wt% Cu), sintered pure Cu nanopaste (100 wt% Cu) and sintered Ag–Cu nanopaste (20–80 wt% Cu) that calculated using Eq. (7). From the plot, the value of CTE that extracted from the region of before transition temperature is larger than those extracted from the region of after transition temperature. Whereby, the sintered pure Ag nanopaste has displayed CTE value of 17.8×10^{-6}/K (before transition temperature) and 10.8×10^{-6}/K (after transition temperatures), and the sintered pure Cu nanopaste has displayed CTE value of 14.3×10^{-6}/K (after transition temperatures) and 4.4×10^{-6}/K (after transition temperatures). For sintered Ag–Cu nanopaste, the value of CTE is decreasing as the loading of Cu is increasing [Fig. 5(c)]. Moreover, its CTE value that extracted from region of before transition temperature ($16.6–14.4 \times 10^{-6}$/K) is also larger than those extracted from the region of after transition temperature ($9.3–5.6 \times 10^{-6}$/K). These results indicate that, beyond the transition temperature, the sintered nanopaste expands much slower if compared to those lower than the transition temperature. This phenomenon is attributed to the presence of pores (more than 48%, depending on the Cu loading [43]) that are able to accommodate the thermal expansion effectively at high temperature [33,34,36,41]. Fig. 6 illustrates the effect of temperature on thermal expansion with the changes of inter-atomic distance and pore size (diameter). To simplify the explanation, only linear thermal expansion (in one dimension) is being used. By increasing the temperature, thermal energy is being absorbed by the atoms and converted into atomic vibration. The effect of vibration may induce increased of inter-atomic distance, where this also translates to the increment in the dimension of the sample. Due to the existence of pores in the sample, the increment of inter-atomic distance will expand towards the empty spaces of the pores. As a result, shrinkage of the pore size may happen in order to absorb the